

UV-Stable Paper Coated with APTES-Modified P25 TiO₂ Nanoparticles

Fei Cheng, Seyed Mani Sajedin and Stephen M. Kelly*

5 *Department of Chemistry, University of Hull, Cottingham Road, Hull, HU6 7RX, UK*

Adam F. Lee

10 *European Bioenergy Research Institute, Aston University, Aston Triangle, Birmingham, B4
7ET, UK*

Andreas Kornherr

15 *Mondi Uncoated Fine Paper, Haidmuehlstrasse 2-4, A-3363 Ulmerfeld-Hausmening, Austria*

Abstract

In order to inhibit the photocatalytic degradation of organic material supports induced by small titania (TiO₂) nanoparticles, highly photocatalytically active, commercially available
20 P25-TiO₂ nanoparticles were first modified with a thin layer of (3-aminopropyl)triethoxysilane (APTES). These APTES-modified P25 TiO₂ nanoparticles were then deposited *and* fixed onto the surface of paper samples *via* a simple, dip-coating process in water at room temperature. The resultant APTES-modified P25 TiO₂ nanoparticle-coated paper samples exhibit much greater stability to UV-illumination than uncoated blank reference paper and very little, or no,
25 photo-degradation in terms of brightness and whiteness, respectively, of the P25-TiO₂-nanoparticle-treated paper is observed. There are many other potential applications for this Green Chemistry approach to protect cellulosic fibres from UV-bleaching in sunlight and to maintain their whiteness and brightness.

30 *Corresponding author: Tel: +44 1482 466347; *E-mail*: s.m.kelly@hull.ac.uk

Keywords: P25 TiO₂ nanoparticles, APTES, UV-stable paper, dip-coating, green chemistry

1 Introduction

35 Titanium dioxide (TiO₂) is a very important industrial material and has been widely used in pigments, paints, cosmetics, photocatalysis and supports. (Chen, Wang, & Chiu, 2007; Gesenhues, 2001; Fernandez-Garcia, Martinez-Arias, Hanson, & Rodriguez, 2004) It has also

been used for anti-reflection coatings, optical coatings and beam splitters due to its high dielectric constant and reflection index. (Samuel, Pasricha, & Ravi, 2005) Titanium dioxide naturally exists in three crystalline polymorphs: anatase, rutile and brookite. The most commonly used forms are anatase and rutile. (Pelton, Geng, & Brook, 2006; Wold, 1993) Both
5 of the anatase and rutile TiO₂ are commonly used in photocatalysis, with anatase TiO₂ showing higher photocatalytic activity. (Linsebigler, Lu, & Yates, 1995) P25 is a commercial TiO₂ powder (EVONIK), which consists of 80% of the anatase phase and 20% of the rutile phase. It has been widely applied in the field of photocatalytic reactions due to its high photocatalytic activity. (Ryu, & Choi, 2008) Unfortunately, the high redox activity of titania can lead to
10 photodegradation of any organic substrate, support, functional material, etc, which will limit its applications in paper, textile, paint and plastic film industries. Selecting large particle size titania (particle size larger 200 nm), using rutile titania and passivated titania nanoparticles with inert shells, such as silica (SiO₂), to form core/shell TiO₂/SiO₂ nanoparticles are the most common method used in attempts to inhibit the photocatalytic effect of TiO₂ and inhibit
15 degradation of the supports. (Furusawa, Honda, Ukaji, Sato, & Suzuki, 2008)

3-Aminopropyltriethoxysilane (APTES) is frequently used as a coupling agent for attaching organic molecules to hydroxylated silicon oxide or metal oxide substrates due to the presence of terminal amine groups. (Kim, Cho, Seidler, Kurland, & Yadavalli, 2010; Pasternack, Amy, & Chabal, 2008) For example, APTES has been applied to link proteins or
20 to promote cell adhesion on TiO₂ surfaces. (Balasundaram, Sato, & Webster, 2006; Filippini, Rainaldi, Ferrante, Mecheri, Gabrielli, Bombace, Indovina, & Santini, 2001)) Adsorption of organic dyes on TiO₂ surfaces has also been reported using APTES as a coupling agent. (Andrzejewska, Krysztafkiewicz, & Jesionowski, 2004) Although in many cases APTES has been applied for specific purposes, disagreements often occur on the dominant conformation
25 or chemical form of APTES at interfaces because they not only depend on the reaction conditions but also on the crystal structures of TiO₂ substrate. (Song, Hildebrand, & Schmuki, 2010; Chen, & Yakovlev, 2010; Ukaji, Furusawa, Sato, & Suzuki, 2007) APTES has not so far, to the authors' best knowledge, been used to deposit and bind TiO₂ nanoparticles to the surface of cellulose or its derivatives.

30 Cellulose is the most abundant, widespread and naturally occurring biopolymer in nature. Alongside its traditional applications in paper and cotton textiles, cellulose is also a very important environmentally friendly, biocompatible and cost-effective, carbon-based resource for the development of novel advanced functional materials. (Habibi, Lucia, & Rojas, 2010) Cellulose is a extensive, linear, mainchain carbohydrate polymer consisting of repeating

β -D-glucopyranose moieties, which are covalently linked through acetal functions between the equatorial OH groups. The presence of a large number of hydrophilic hydroxyl groups (Klemm, Heublein, Fink, & Bohn, 2005; Roy, Semsarilar, Guthrie, & Perrier, 2009) can promote the nucleation and growth of inorganic phases at the cellulose fibre surface and thus facilitate the production of organic/inorganic nanocomposites. (Pinto, Marques, Barros-Timmons, Trindade, & Neto, 2008; Li, Chen, Hu, Shi, Shen, Zhang, & Wang, 2009; Iguchi, Ichiura, Kitaoka, & Tanaka, 2003)

Protection of cellulosic textiles against different kinds of degradation and the creation of new advantageous functions can be realised by coating of the textiles with silica sols with nanoparticle diameters smaller than 50 nm. (Mahltig, Haufe, & Bottcher, 2005). The surface of vegetable cellulose fibres has been modified, for example, with a nanoparticle-functionalised siloxane coating first using the hydrolysis of tetraethoxysilane (TEOS), octyltrimethoxysilane (OTMS) or polydimethylsiloxane (PTMS), followed then by layer-by-layer deposition of previously synthesized titanium dioxide nanoparticles. (Goncalves, Marques, Pinto, Trindade, & Neto, 2009) Morphologically well-defined silica nanoparticles have been successfully deposited at cellulose fibre surfaces *via* a polyelectrolytes layer-by-layer approach. (Pinto, Marques, Barros-Timmons, Trindade, & Neto, 2008)

In this report, commercially available, highly photochemically active and strongly UV-absorbing P25 TiO₂ nanoparticles (EVONIK) have been modified to form a strongly UV-absorbing, but non-photo-catalytically active, coating on the surface of cellulose paper in order to significantly improve its resistance to UV-degradation in terms of maintaining the original brightness and whiteness of paper samples under standard, commercial UV-illumination test conditions. In a simple, two-step process the surface of small, photo-active titania nanoparticles was first modified with a thin coating of APTES to produce deactivated, APTES-coated TiO₂ nanoparticles, which were then deposited *and* fixed on the surface of paper simply using a very simple, water-based dip-coating procedure at room temperature. The APTES-modified TiO₂ nanoparticles protect the paper from photochemical bleaching as far as possible under standard UV-illumination test conditions. No impact or spray coating techniques, chemical binders, surfactants, dispersants or a post-treatment curing step are required in this two-step process. The presence of additional amine and silane groups present in the APTES coating covering the surface of the APTES-modified TiO₂ nanoparticles should promote attachment *and* fixation to the many hydroxyl-groups present on the surface of the cellulose fibres. The APTES-modified TiO₂ nanoparticles are prepared in a simple fashion at a relatively low reaction temperature.

The structural and mechanical properties of the cellulose fibres will not be impaired by the presence of the APTES-modified TiO₂ nanoparticles, whose presence just on the outer surface, not in the core, of the fibre will ensure a high effective absorption of UV-light. A much lower loading of nanoparticles is required using this surface-based approach than dispersing nanoparticles in the bulk fibre mixtures used to prepare paper, fabrics, textiles, etc., which is advantageous in terms of minimising contamination of the environment with nanoparticles.

2 Experimental

2.1 Materials and characterization methods

10 TiO₂ P25 with approximately 80/20 of anatase and rutile TiO₂ was provided by EVONIK. (3-aminopropyl)triethoxysilane [APTES, (C₂H₅O)₃Si(CH₂)₃NH₂] and xylene were supplied by Aldrich and used as received. The paper samples, which are 1 mm thick, and do not possess a surface coating such calcium carbonate or china clay, were provided by Mondi Uncoated Fine Paper, Austria. Acetone was sourced from Fisher Scientific, UK, and used as received.

15 Fourier transform infrared spectra were recorded on a Nicolet Magna-500 FTIR spectrometer. X-ray powder diffraction (XRD) analyses were performed on a SIEMENS D5000 Instrument. Scanning electron microscopy (SEM) images were obtained using Carl Zeiss SMT 'EVO60' SEM microscope operating at 20 kV and EDX data were obtained using an Oxford Instruments 'INCA' Energy Dispersive X-ray Spectrometer. Transmission electron
20 microscopy (TEM) was collected using a Jeol 2010 TEM running at 200kV. Images were obtained with a Gatan Ultrascan 4000 digital camera. Solid samples were prepared by suspension in distilled water and 5 µl aliquots of a suitable dilution dropped onto carbon coated copper grids. The BET surface area and pore size diameter of powders was calculated from nitrogen adsorption/desorption isotherms at 77 K using a Micromeritics three star 3000
25 instrument. The whiteness of the standard paper samples and the APTES-modified TiO₂ nanoparticle paper samples was measured with a standard whiteness tester (Lorentzen&Wettré, Elrepho). The brightness of these samples was determined before and after the suntest (Suntest XLS₊; ATLAS Material Testing Solutions). The suntester allows irradiation of paper samples with a xenon lamp under accurate, repeatable conditions (i.e. 90 min, 500 W, and 2700 kJ/m²).
30 XPS was performed on a Kratos Axis HSi X-ray photoelectron spectrometer fitted with a charge neutraliser and magnetic focusing lens employing Al K_α monochromatic radiation (1486.7 eV). Surface elemental analysis was undertaken on Shirley background-subtracted

spectra applying the appropriate instrument and element specific response factors. Spectral fitting was conducted using CasaXPS version 2.3.14, with binding energies corrected to the C 1s peak at 284.5 eV and high-resolution C 1s, O 1s, N 1s, Si 2p and Ti 2p XP spectra fitted using a common Gaussian/Lorentzian peak shape. Errors were estimated by varying the Shirley background subtraction procedure across reasonable limits and re-calculating fits. The photocatalytic activity of the P25 TiO₂ and APTES modified TiO₂ was evaluated in terms of the degradation of Rhodamine B. (Ren, Chen, Zhang, & Wu, 2010) P25 TiO₂ or APTES modified TiO₂-powder (10 mg) was suspended in 10 mL of water and then 10 mL of Rhodamine B solution (20 mg/L) was added to the suspension solution. The UV irradiation was carried out under a UV light at 365 nm for 30 min. The suspension solutions were centrifuged at 10000 rpm for 15 min. The Rhodamine B content in the solutions was determined by UV-Vis analysis in the range between 300 and 700 nm using a Perkin Elmer Lambda 25 spectrometer.

2.2 Modification of TiO₂ surfaces with APTES (TiO₂-APTES)

APTES (1.5 mL) was added to a stirred suspension of P25 TiO₂ nanoparticles (0.5 g) in xylene (50 mL). After allowing the reaction mixture to react at 50 °C for 10 h, a white powder was obtained by centrifugation of the cooled the reaction mixture, which was then washed with xylene and then twice with acetone followed by drying under vacuum overnight.

20

2.3 Coating of papers with APTES modified TiO₂ nanoparticles

The APTES-stabilised P25 TiO₂ nanoparticle powder was added to distilled water (20mL) and sonicated for 15 min to produce a stable, aqueous colloidal solution of APTES-stabilised P25 TiO₂ nanoparticles. A sample of commercial uncoated paper (0.7 g) was then immersed in the aqueous colloidal solution. After sonication for 15 min, the paper sample coated with APTES-stabilised P25 TiO₂ nanoparticles was washed carefully with copious amounts of distilled water and dried under vacuum overnight.

3 Results and Discussions

3.1 Modification of P25 TiO₂ nanoparticles with APTES

The IR spectra of P25 TiO₂ nanoparticles and APTES-modified P25 TiO₂ nanoparticles shown in Fig. 1 reveal a small peak at 1640 cm⁻¹ and large, broad peak between 3450 and 3200 cm⁻¹, which are due to stretching vibrations of absorbed water, as well as surface hydroxyl (–OH) groups present on the surface of the nanopowder. (Chen, & Yakovlev, 2010) The broad peak between 600–400 cm⁻¹ can be assigned to the Ti–O–Ti bond. Compared with P25 TiO₂ nanoparticles, the APTES-modified P25 TiO₂ nanoparticles show a weak band at 2923 cm⁻¹, which can be assigned to alkyl groups [–(CH₂)_n–] present in APTES. The new absorption band at 1561 cm⁻¹ is attributable to a NH₂ scissor vibration, suggesting the presence of the amino groups of APTES molecules in the terminal of the propyl chain. (Pasternack, Amy, & Chabal, 2008) Furthermore, the peak at around 1024 cm⁻¹ can be assigned to the stretch vibration of Ti–O–Si moieties, formed by a condensation reaction between silanol groups of APTES and hydroxyl groups present on the surface TiO₂ nanoparticles. (Ukaji, Furusawa, Sato, & Suzuki, 2007) In addition, the broad band at around 1116 cm⁻¹ is probably attributable to the stretch vibration of Si–O–Si, produced by the condensation reactions between silanol groups. (Chen, & Yakovlev, 2010) All these facts suggest that APTES has been successfully attached as a thin film to the surface of the P25 TiO₂ nanoparticles.

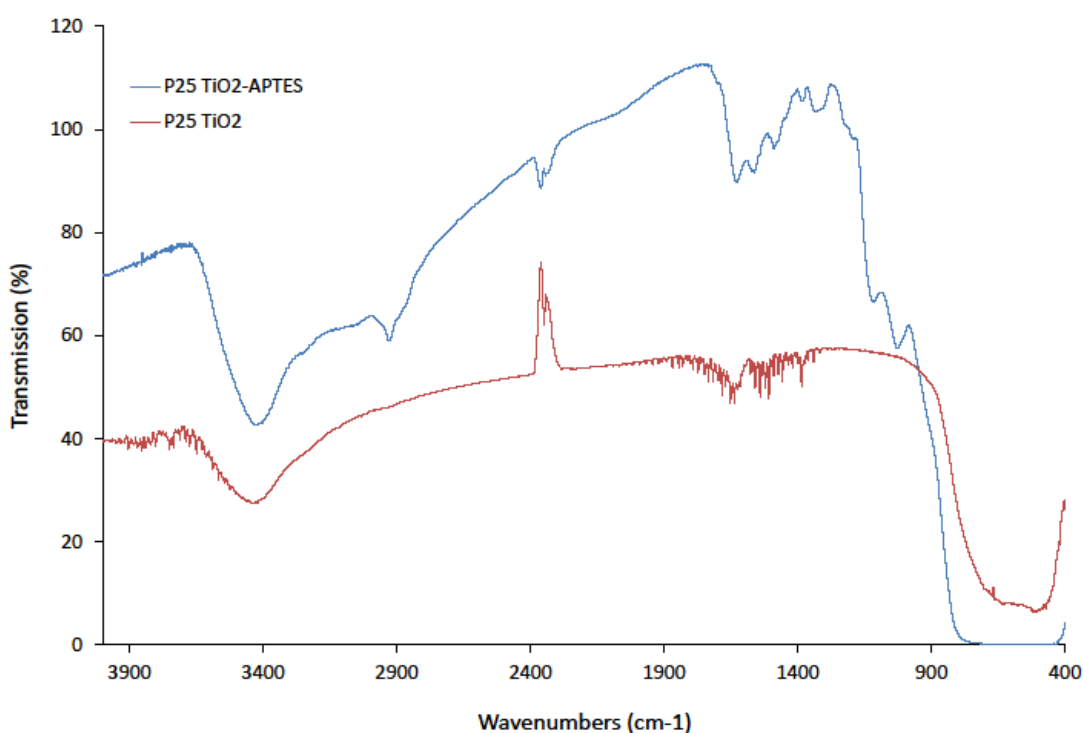


Fig. 1. Infrared spectra of commercially available P25 TiO₂ nanoparticles and APTES-modified P25 TiO₂ nanoparticles.

5 XPS spectra of the P25 TiO₂ nanoparticles and corresponding APTES-modified P25 TiO₂ nanoparticles are shown in Fig. 2. In comparison with the survey spectrum of the P25 TiO₂ nanoparticles (Figure 2A), the APTES-modified P25 TiO₂ nanoparticles exhibit new peaks corresponding to N 1s and Si 2p photoemission features, clearly indicating surface modification of the titanium oxide surface by an aminosilane. Fig. 2B-2F shows the corresponding high resolution C 1s, O 1s, Si 2p, N 1s and Ti 2p XP spectra. **The C1s spectra were deconvoluted using three components, C1, C2 and C3. The C1, C2 and C3 peaks in the C 1s spectrum of P25 TiO₂ nanoparticles at 284.41 (82.7 %), 286.04 (9.44 %) and 288.15 (7.86 %) (Table 1) are assigned to CH_x, C-O and C=O bonds respectively, associated with adventitious hydrocarbon resulting from sample preparation and handling. (Arranz, Palacio, Garcia-Fresnadillo, Orellana, Navarro, & Munoz, 2008) APTES modified titania also exhibits three carbon components at 284.84 (68.33 %), 286.20 (18.51 %) and 288.16 (13.17 %), which are attributed to CH_x/C-C/C-Si, C-N/C-O and C=O functions respectively. (Song, Hildebrand, & Schmuki, 2010) The C3 component likely arises from organic residues during sample handling/transportation since APTES does not contain a carbonyl function. Such high binding energy carbon moieties have also been reported during the APTES modification of GaN and**

10

15

20

amorphous TiO₂ surfaces. (Song, Hildebrand, & Schmuki, 2010; Song, Hildebrand, & Schmuki, 2010) The O 1s spectrum also exhibited a new peak at 532.13 eV after APTES modification, ascribed to O-Si-R surface species. The presence of a sharp peak at 102.13 eV in the Si 2p clearly evidences APTES attachment to the TiO₂ nanoparticle surface, with surface compositional analysis showing that the APTES modified titania possess 17.2 atom% silicon (Table 2). Three new N 1s peaks were also observed following APTES modification at 339.18, 400.61 and 401.61 eV. The 339.18 eV component is assigned to terminal NH₂ groups in the APTES coating of the P25 TiO₂ nanoparticles, whereas the peaks at 400.61 and 401.61 eV are possibly due to hydrogen-bonded NH₂ or protonated amino-groups (-NH₃⁺). (Song, Hildebrand, & Schmuki, 2010)

The possible modes of interactions of APTES, which has two distinct terminal functional groups: the hydrolysable silane (-Si(OR)₃) group and the amino- (-NH₂) group, with the TiO₂ nanoparticle surface are shown in Fig. 3. (Ukaji, Furusawa, Sato, & Suzuki, 2007; Acres, Ellis, Alvino, Lenahan, Khodakov, Metha, & Andersson, 2012) If the silane groups react with hydroxyl groups present on the TiO₂ nanoparticle surface to form a silanized surface, as shown in Fig. 3a-d, then free terminal -NH₂ groups, which project away from the TiO₂ nanoparticle surface, can be observed at 399.18 eV (normal attachment). On the other hand, if the -NH₂ groups are attached to the surface through hydrogen bonding, or protonated amine (-NH₃⁺) ionic bonding, with the hydroxyl groups on the TiO₂ nanoparticle surface, as shown in Fig. 3 (e) and 3(f), the N 1s peak will appear at higher energy (~ 400.9 eV) (reverse attachment). Since the contribution of the peak at 399.18 eV is 60.42 % and much higher than that of the peaks at 400.61 eV (24.92 eV) and 401.61 (14.67 eV), APTES appears to be mainly attached by silanized bonding with free terminal NH₂ projecting away from the nanoparticle surface, which would be similar to similar to previously reported behaviour. (Pasternack, Amy, & Chabal, 2008; Arranz, Palacio, Garcia-Fresnadillo, Orellana, Navarro, & Munoz, 2008; Vandenberg, Bertilsson, Liedberg, Uvdal, Erlandsson, Elwing, & Lundstrom, 1991)

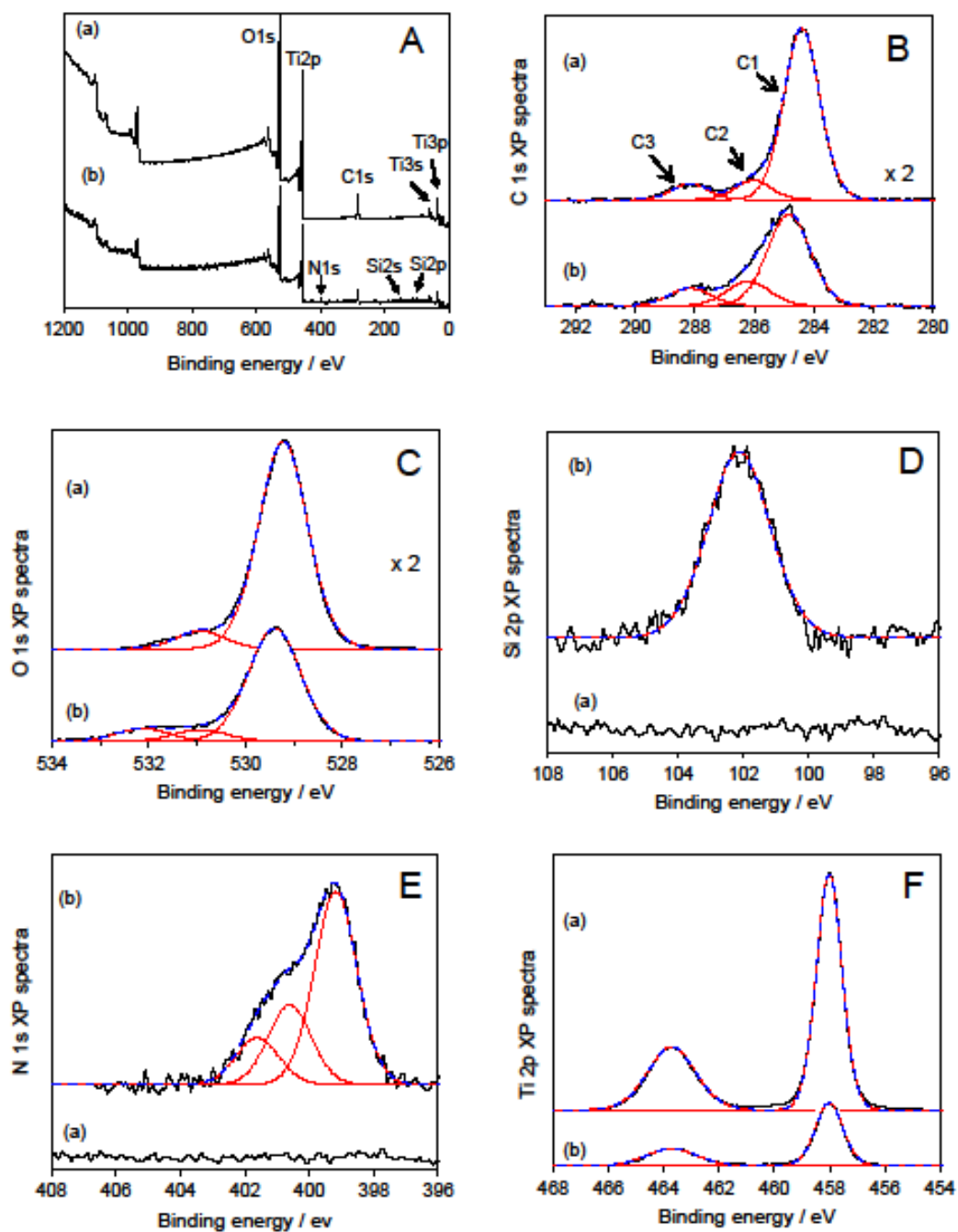


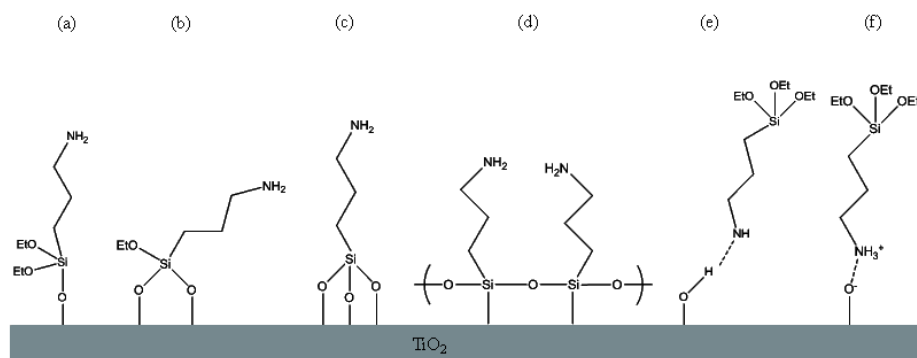
Fig. 2. (A) XPS survey spectra and (B) C 1s, (C) O 1s, (D) Si 2p, (E) N 1s and (F) Ti 2p high-resolution spectra of (a) commercially available, untreated P25 TiO₂ nanoparticles and (b) APTES-modified P25 TiO₂ nanoparticles.

Table 1 XPS surface analysis of P25 TiO₂ and APTES modified TiO₂ nanoparticles

	TiO ₂		TiO ₂ – APTES	
	Binding energy /ev	%	Binding energy /ev	%
Ti 2p	458.00		458.00	
	?		?	
O 1s	529.23	92.01	529.40	82.03
	530.94	7.99	530.93	8.63
			532.13	9.34
C 1s	284.41	82.70	284.84	68.33
	286.04	9.44	286.20	18.51
	288.15	7.86	288.16	13.17
N 1s			399.18	60.42
			400.61	24.92
			401.61	14.67
Si			102.13	

5 **Table 2** XPS surface elemental analysis for APTES-modified P25 TiO₂ nanoparticles.

Element	%
Ti	18.88
O	51.14
C	23.16
N	3.56
Si	3.25



10 **Fig. 3.** Possible surface interactions and potential modes of chemical bonding between a TiO₂ nanoparticle surface and (3-aminopropyl)triethoxysilane (APTES).

The active surface area of the APTES-modified P25 TiO₂ nanoparticles as determined using absorption experiments and BET analysis is 47.5 m²/g, which is marginally lower (2.5 m²/g) than that of the untreated P25 TiO₂ nanoparticles (50.0 m²/g), due to the coating of APTES on the surface of P25 TiO₂ nanoparticle powder. The photocatalytic activity of the P25 TiO₂ and APTES modified TiO₂ powder was tested by adding samples of the untreated and treated P25 TiO₂ nanoparticles to a Rhodamine solution followed by UV-irradiation at 365 nm for 30 min. The UV/vis analysis shows that 51.8% of Rhodamine is degraded by the APTES-modified P25 TiO₂ nanoparticles, compared with 58.5% of Rhodamine degradation by the untreated P25 TiO₂ nanoparticles (Fig. 4). The lower photocatalytic activity of APTES-modified P25 TiO₂ nanoparticles further supports the assumption that the surfaces of treated P25 TiO₂ nanoparticles have indeed been coated with APTES. However, the TEM images of P25 TiO₂ and APTES APTES-modified P25 TiO₂ nanoparticles show no significant differences in size or shape of the nanoparticles before and after treatment (not show), which indicates that the APTES coating present on the TiO₂ surface is very thin, as could be reasonably expected.

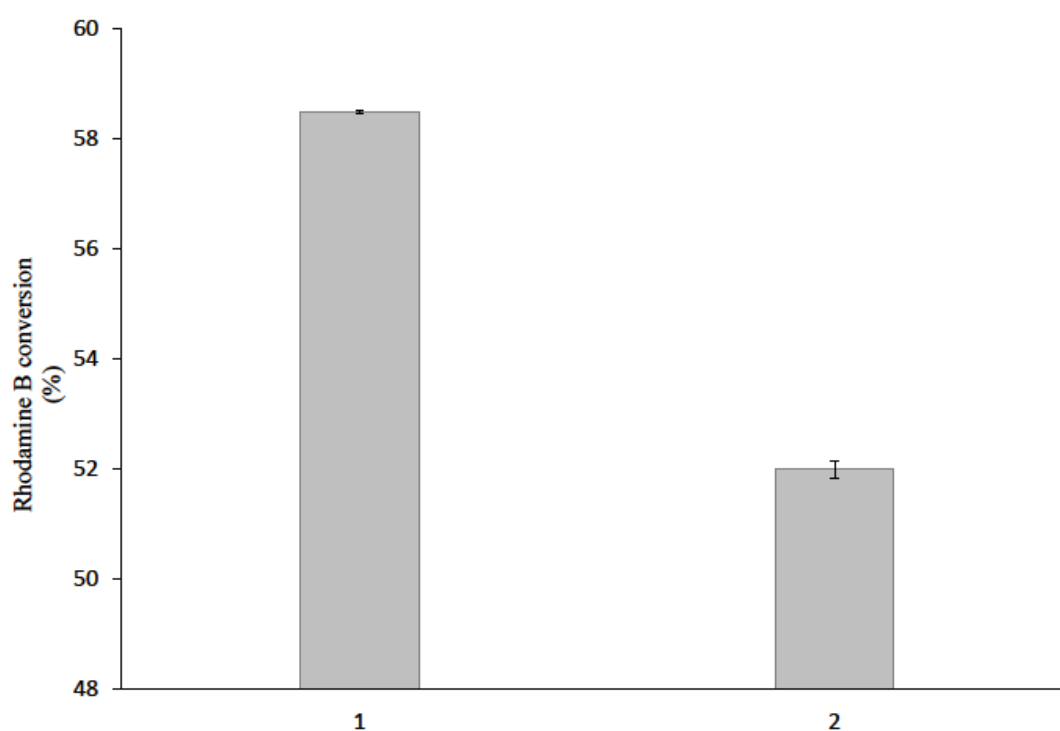


Fig. 4. Rhodamine B photodegradation by (1) commercially available P25 TiO₂ nanoparticles and (2) APTES-modified P25 TiO₂ nanoparticles after 30 min UV-irradiation.

3.2 Deposition of APTES-modified P25 TiO₂ nanoparticles on paper

The APTES-modified P25 TiO₂ nanoparticles have free terminal amino-groups (normal attachment of -NH₂ groups) and hydrolysable silane groups (reverse attachment of -Si(OR)₃ groups). Therefore, the presence of free terminal NH₂ groups can facilitate the attachment of the APTES-modified P25 TiO₂ nanoparticles to the cellulose fibres through hydrogen bonding between amino- or protonated amino- (-NH₃⁺) groups with hydroxyl groups present the surface on the surface of the cellulose fibres. The silane groups will also react with the hydroxyl groups on cellulose fibres to fix P25 TiO₂ nanoparticles onto the surface of the cellulose paper. These interactions and chemical reactions ensure the fixation of the APTES-modified P25 TiO₂ nanoparticles on the surface of the cellulose fibres, that cannot removed by repeated washing with copious amounts of water.

Figure 5 shows the XRD patterns of the paper substrate and the paper coated with the APTES-modified P25 TiO₂ nanoparticles. It can be seen that beside a strong peak attributable to cellulose at $2\theta = 23^\circ$, a weak anatase titania peak attributable to TiO₂-P25 can also be observed. However, peaks attributable to the minority rutile polymorph present in the standard, commercially available P25 TiO₂ nanoparticles are probably too weak to be observed. SEM images also show that the surfaces of the cellulose fibres are covered with a coating of APTES-modified P25 TiO₂ nanoparticles and no nanoparticles can be observed between the fibres of cellulose, see Fig. 6. In contrast, the untreated P25 TiO₂ nanoparticles are mainly located between the fibres of the cellulose, rather than being attached to the surface of the fibres (Fig. 6).

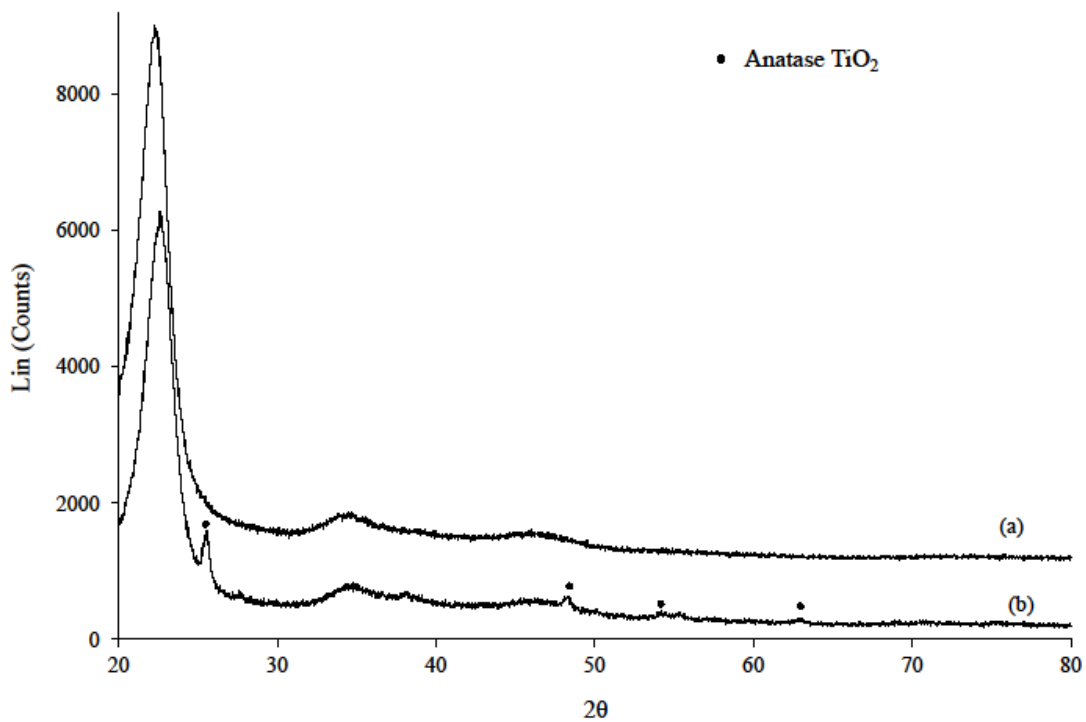


Fig. 5. XRD pattern of (a) cellulose paper and (b) cellulose paper coated with APTES-modified P25 TiO₂ nanoparticles.

5

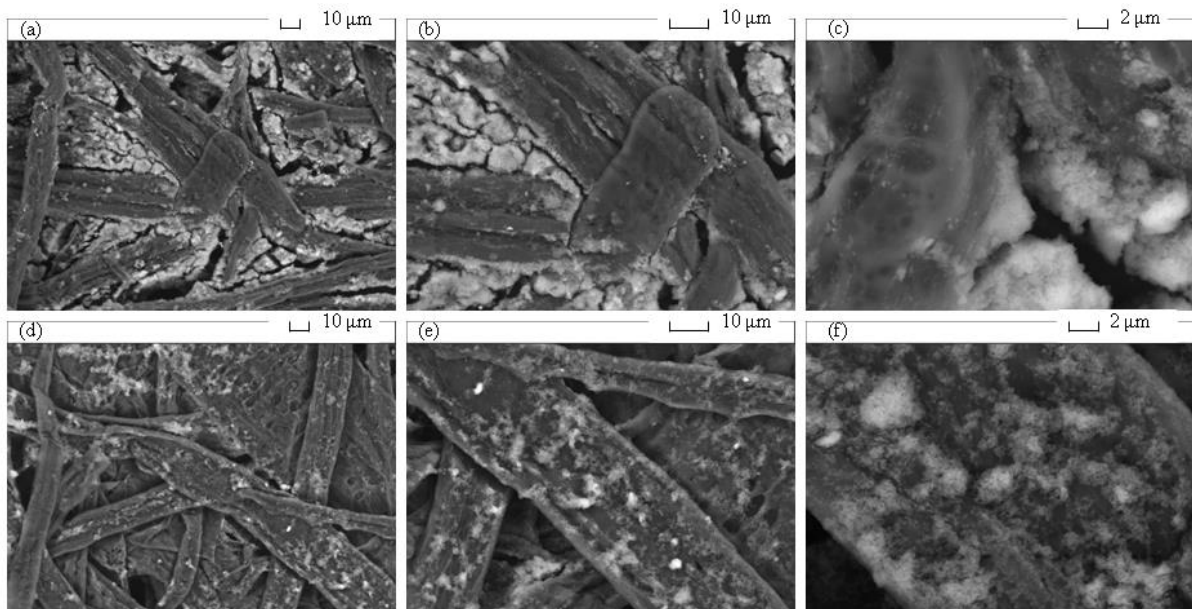


Fig. 6. SEM images of cellulose papers coated with (a, b and c) commercially available P25 TiO₂ nanoparticles and (d, e and f) APTES-modified P25 TiO₂ nanoparticles.

10

The ISO-brightness determined for the blank reference paper and the paper samples coated either with untreated P25 TiO₂ nanoparticles or APTES-modified P25 TiO₂ nanoparticles, before and after illumination with UV-light in the standard xenon UV-stability test, is shown in Fig. 7(a). It can be seen that the brightness of the blank paper reference is sharply reduced after illumination with UV radiation in the standard xenon test. The reduction in brightness is even more significant for the paper samples coated with untreated P25 TiO₂ nanoparticles. In contrast, there is only a marginal reduction in the brightness of the paper samples coated with APTES-modified P25 TiO₂ nanoparticles. It seems reasonable to assume that the small reduction in the brightness of the APTES-modified P25 TiO₂ nanoparticle coated paper sample after the xenon UV-test is attributable to the fact that the photo-catalytically active titania nanoparticles have been coated effectively with a thin, inert layer of APTES, which passivates their surface and thereby inhibits their inherent photocatalytic activity. The value for the CIE-whiteness of the cellulose paper coated with APTES-modified P25 TiO₂ nanoparticles is slightly higher than that of either the blank paper reference and that of the P25 TiO₂-nanoparticle-coated paper sample, see Fig. 7(b). In contrast to the sharp reduction in the whiteness of the blank paper reference sample and the P25 TiO₂ nanoparticle coated paper sample, no reduction in whiteness can be observed for the paper coated with the APTES-modified P25 TiO₂ nanoparticles, after the standard xenon UV-stability test.

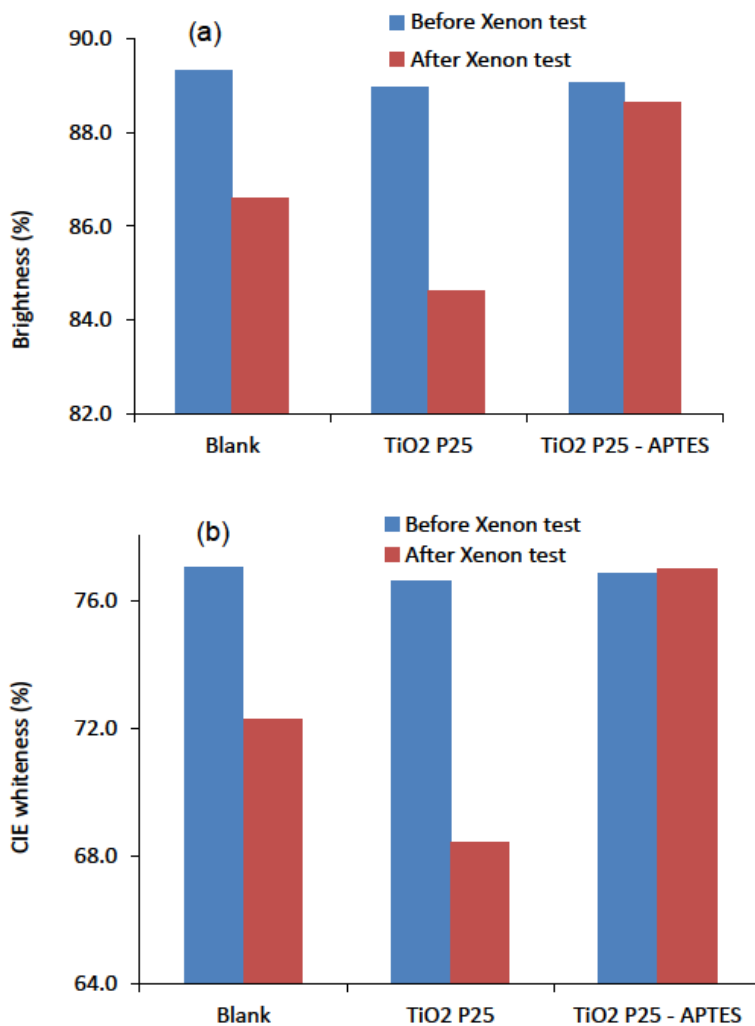


Fig. 7. (a) ISO-brightness and (b) CIE whiteness of blank reference paper and the paper samples coated either with untreated P25 TiO₂ nanoparticles or APTES-modified P25 TiO₂ nanoparticles before and after the UV-stability test.

5

3.3 Conclusion

A simple dip-coating procedure has been successfully applied to attach APTES-modified, commercially available P25 TiO₂ nanoparticles onto the surface of standard, commercial **uncoated** paper samples. The presence of free terminal NH₂ groups and hydrolysable silane groups in the APTES-modified P25 TiO₂ nanoparticles contributes to the attachment of TiO₂ onto the surface of the constituent fibres of the paper samples. The presence of the APTES coating between the titania nanoparticles and cellulose fibres effectively inhibits the strong photocatalytic degradation effect of the titania nanoparticles. The paper samples coated with APTES-modified P25 TiO₂ nanoparticles exhibit a significantly higher stability to UV-bleaching than that of the untreated commercial paper reference.

Acknowledgements

We thank the European Union Seventh Framework Programme (FP7/2007-2013) for financial support under Grant Agreement Number 214653 (SURFUNCELL project), and the EPSRC for the award of a Leadership Fellowship (EP/G007594/3) to AFL. Mrs A Lowry, Mr A Sinclair, Mr R Knight and Mr M. Isaacs are thanked for providing TEM, SEM, ICP and XPS analyses, respectively.

References

- 10
Acres, R. G., Ellis, A. V., Alvino, J., Lenahan, C. E., Khodakov, D. A., Metha, G. F., & Andersson, G. G.(2012). Molecular Structure of 3-Aminopropyltriethoxysilane Layers Formed on Silanol-Terminated Silicon Surfaces. *Journal of Physical Chemistry C*, *116*(10), 6289-6297.
- 15 Andrzejewska, A., Krysztafkiewicz, A. & Jesionowski, T. (2004). Adsorption of organic dyes on the aminosilane modified TiO₂ surface. *Dyes and Pigments*, *62*(2), 121-130.
- Arranz, A., Palacio, C., Garcia-Fresnadillo, D., Orellana, G., Navarro, A., & Munoz, E.(2008). Influence of surface hydroxylation on 3-aminopropyltriethoxysilane growth mode during chemical functionalization of GaN surfaces: An angle-resolved X-ray photoelectron spectroscopy study. *Langmuir*, *24*(16), 8667-8671.
- 20 Balasundaram, G., Sato, M., & Webster, T. J. (2006). Using hydroxyapatite nanoparticles and decreased crystallinity to promote osteoblast adhesion similar to functionalizing with RGD. *Biomaterials*, *27*(14), 2798-2805.
- 25 Chen, H.J., Wang, L., & Chiu, W.Y. (2007). Chelation and solvent effect on the preparation of titania colloids. *Materials Chemistry and Physics*, *101*(1), 12-19.
- Chen, Q., & Yakovlev, N. L. (2010) Adsorption and interaction of organosilanes on TiO₂ nanoparticles. *Applied Surface Science*, *257*(5), 1395-1400.
- Fernandez-Garcia, M., Martinez-Arias, A., Hanson, J. C., & Rodriguez, J. A. (2004). *Nanostructured oxides in chemistry: Characterization and properties. Chemical Reviews*, *104*(9), 4063-4104.
- 30 Filippini, P., Rainaldi, C., Ferrante, A., Mecheri, B., Gabrielli, G., Bombace, M.,

- Indovina, P. L., & Santini, M. T. (2001). Modulation of osteosarcoma cell growth and differentiation by silane-modified surfaces. *Journal of Biomedical Materials Research*, 55(3), 338-349.
- 5 Furusawa, T., Honda, K., Ukaji, E., Sato, M., & Suzuki, N. (2008). The microwave effect on the properties of silica-coated TiO₂ fine particles prepared using sol-gel method. *Materials Research Bulletin*, 43(4), 946-957.
- Gesenhues, U. (2001). Calcination of metatitanic acid to titanium dioxide white pigments. *Chemical Engineering & Technology*, 24(7), 685-694.
- 10 Goncalves, G., Marques, P., Pinto, R. J. B., Trindade, T., & Neto, C. P. (2009). Surface modification of cellulosic fibres for multi-purpose TiO₂ based nanocomposites. *Composites Science and Technology*, 69(7-8), 1051-1056.
- Habibi, Y., Lucia, L.A., & Rojas, O. J. (2010). Cellulose nanocrystals: chemistry, self-assembly, and applications. *Chemical Reviews*, 110(6), 3479-3500.
- 15 Iguchi, Y., Ichiura, H., Kitaoka, T., & Tanaka, H. (2003). Preparation and characteristics of high performance paper containing titanium dioxide photocatalyst supported on inorganic fiber matrix. *Chemosphere*, 53(10), 1193-1199.
- Kim, J., Cho, J., Seidler, P. M., Kurland, N. E., & Yadavalli, V. K. (2010). Investigations of chemical modifications of amino-terminated organic films on silicon substrates and controlled protein immobilization. *Langmuir*, 26(4), 2599-2608.
- 20 Klemm, D., Heublein, B., Fink, H. P., & Bohn, A. (2005). Cellulose: Fascinating biopolymer and sustainable raw material. *Angewandte Chemie-International Edition*, 44(22), 3358-3393.
- Li, X., Chen, S. Y., Hu, W. L., Shi, S. K., Shen, W., Zhang, X., & Wang, H. P. (2009). In situ synthesis of CdS nanoparticles on bacterial cellulose nanofibers. *Carbohydrate*
- 25 *Polymers*, 76(4), 509-512.
- Linsebigler, A.L., Lu, G.Q., & Yates, J.T. (1995). Photocatalysis on TiO₂ surface - principles, mechanisms, and selected results. *Chemical Reviews*, 95(3), 735-758.
- Mahltig, B., Haufe, H., & Bottcher, H. (2005). Functionalisation of textiles by inorganic sol-gel coatings. *Journal of Materials Chemistry*, 15(41), 4385-4398.
- 30 Pasternack, R.M., Amy, S.R., & Chabal, Y. J. (2008). Attachment of 3-(aminopropyl)triethoxysilane on silicon oxide surfaces: dependence on solution temperature. *Langmuir*, 24(22), 12963-12971.
- Pelton, R., Geng, X. L., & Brook, M. (2006). Photocatalytic paper from colloidal TiO₂ - fact or fantasy. *Advances in Colloid and Interface Science*, 127(1), 43-53.

- Pinto, R. J. B., Marques, Paap, Barros-Timmons, A. M., Trindade, T., & Neto, C. P. (2008). Novel SiO₂/cellulose nanocomposites obtained by in situ synthesis and via polyelectrolytes assembly. *Composites Science and Technology*, 68(3-4), 1088-1093.
- Ren, Y. A., Chen, M., Zhang, Y., & Wu, L. M. (2010).
5 Fabrication of Rattle-Type TiO₂/SiO₂ Core/Shell Particles with Both High Photoactivity and UV-Shielding Property. *Langmuir*, 26(13), 11391-11396.
- Roy, D., Semsarilar, M., Guthrie, J. T., & Perrier, S. (2009). *Cellulose modification by polymer grafting: a review. Chemical Society Reviews*, 38(7), 2046-2064.
- Ryu, J., & Choi, W. (2008). Substrate-specific photocatalytic activities of TiO₂ and
10 multiactivity test for water treatment application. *Environmental Science & Technology*, 42(1), 294-300.
- Samuel, V., Pasricha, R., & Ravi, V. (2005). Synthesis of nanocrystalline rutile. *Ceramics International*, 31(4), 555-557.
- Song, Y.-Y., Hildebrand, H., & Schmuki, P. (2010). Optimized monolayer grafting of
15 3-aminopropyltriethoxysilane onto amorphous, anatase and rutile TiO₂. *Surface Science*, 604(3-4), 346-353.
- Ukaji, E., Furusawa, T., Sato, M., & Suzuki, N. (2007). The effect of surface modification with silane coupling agent on suppressing the photo-catalytic activity of fine TiO₂ particles as inorganic UV filter. *Applied Surface Science*, 254(2), 563-569.
- 20 Vandenberg, E. T., Bertilsson, L., Liedberg, B., Uvdal, K., Erlandsson, R., Elwing, H., & Lundstrom, I. (1991). Structure of 3-aminopropyl triethoxysilane on silicon - oxide. *Journal of Colloid and Interface Science*, 147(1), 103-118.
- Wold, A. (1993). Photocatalytic properties of TiO₂. *Chemistry of Materials*, 5(3), 280-283.